Supporting Information -

Determination of the positions and orientations of concentrated rod-like colloids from 3D microscopy data

T. H. Besseling,[*] M. Hermes,[†] A. Kuijk, B. de Nijs, T.-S.
Deng, M. Dijkstra, A. Imhof, and A. van Blaaderen[‡]

Soft Condensed Matter, Debye Institute for NanoMaterials Science,

Utrecht University, Princetonplein 1,

NL-3584 CC Utrecht, the Netherlands

(Dated: October 13, 2014)

[*] Both authors contributed equally; t.h.besseling@uu.nl

[†] Both authors contributed equally; michielhermes@colloids.nl

[‡] a.vanblaaderen@uu.nl; www.colloid.nl

A.   Generation of particle coordinates

To construct time-series of 3D test-data, we first generated artificial 3D particle trajectories. We used a single-particle approach where we generated random (orientational) displacements for a set of independent particles and did not allow particles to interact. For the first set of trajectories, we fixed 25 particles on a 5x5x1 hexagonal lattice in 3D. For each particle a unit vector $\mathbf{u}_0$ was initialized, which represented the principal axis of the particle. The particles were not allowed to translate, however, they were able to rotate with a fixed diffusion coefficient D_r. The reduced rotational diffusion coefficient is given by $D_r^* = D_r t_s$ (in rad^2) with t_s the time-step. Particles were rotated by first randomly selecting rotation angles α, β and γ from a Gaussian distribution with $\sigma_i = \sqrt{2D_r^*}$. Then, the particles were rotated by applying the rotation matrices $\mathbf{u} = \mathbf{R}_x(\alpha)\mathbf{R}_y(\beta)\mathbf{R}_z(\gamma)\mathbf{u}_0$, as is described in detail in Ref. **?** . For the second set of trajectories, we generated 36 trajectories of a single particle that could diffuse freely in all three dimensions. To this end, displacements $\Delta\mathbf{r}$ were drawn from a Gaussian distribution with standard deviation $\sigma_i = \sqrt{2D_t^*}$. Here, we define $D_t^* = D_t t_s/d^2$, with D_t the rotationally averaged translational diffusion coefficient, t_s the timestep and d the particle diameter. The centre-of-mass of the particle was displaced by $\mathbf{r} = \mathbf{r_0} + \Delta\mathbf{r}$. The particle was rotated as before with a fixed rotational diffusion coefficient D_r^*.

B.   The effect of varying the point spread function and noise on particle fitting accuracy

For the first set of particles (fixed on a hexagonal lattice) we used $D_r^* = 0.0025$ rad^2. We generated 3D image stacks of 200 x 163 x 37 pixels for every timestep (1000 timesteps in total). The particles that we generated had a length of $l = 25$ pixels and diameter $d = 7$ pixels in an xy-image. To approximate the effect of the PSF we used a fixed $\sigma_x/d = \sigma_y/d$ = 0.3, representing a constant resolution in the xy direction, with σ_i the standard deviation of the Gaussian kernel and d the diameter of the particle. In the vertical direction we used σ_z/d = 0.3, 0.6 and 0.9. Figs. S1a-c show xz-views of this decrease in z-resolution. Typical rod-like particles used in our experiments have a length $l \sim 3~\mu$m and a fluorescent diameter $d_{fl} \sim 300$ nm. The FWHM of the Gaussian kernels in the z-direction therefore

correspond to $2\sqrt{2\ln 2}\,\sigma_z = 212$ nm, 424 nm and 636 nm respectively. The resolution of our microscope, which we measured to be 190 nm in the lateral (xy) direction and 490 nm in the axial (z) direction [?], is within this range. In Figs. S1d-f we show increasing noise levels, obtained by adding Gaussian noise with standard deviation $\sigma_n = 0.09$, 0.18 and 0.27. These levels resulted in a signal-to-noise ratio (SNR) of 11.2, 3.8 and 1.7 respectively, which corresponds to typical SNR values of the confocal microscopy images that we used for particle tracking. Notice the strong similarity between Figs. S1d-f and Figs. 2d-e in the main paper. In Fig. S1g, we show a test-image with $\sigma_z/d = 0.9$ and $\sigma_n = 0.27$, in Fig. S1h the same image after filtering and in Fig. S1i the particle fitting as indicated by the magenta outline. Fig. S1j and Fig. S1k show the 3D reconstruction with RGB colours indicating particle orientation.

After identification of the orientations in each frame separately, we determined particle trajectories with existing IDL based routines [?]. Fig. S1l shows the calculated mean squared angular displacement (MSAD) for decreasing resolution and increasing noise levels. We obtained the correct D_r^* for all five test cases, as shown by the data-collapse with the theoretical result $4\,D_r\,t$ (black dashed dotted line) for $\Delta t/t_s > 10$. The (coloured) continuous lines are fits to equation (6) (main paper). As expected, the error in the determination of the main axis of the rod (ϵ_r) increases with increasing noise level, as indicated in the figure and shown in Table I in the main paper.

To further test for any biases in our algorithm, we generated 3D test-images of single, freely diffusing particles with imposed diffusion coefficients $D_t^* = 0.01$ and $D_r^* = 0.005$ rad^2. The particles were initially randomly oriented. We constructed 2000 time-frames of 3D image-stacks and convolved them with a Gaussian kernel with standard deviation $\sigma_x/d = \sigma_y/d = 0.3$ and $\sigma_z/d = 0.6$. We also added Gaussian noise with $\sigma_n = 0.09$ to the images. The particles had a length $l = 25$ pixels and a diameter $d = 7$ pixels. To test for a possible pixel-bias of the algorithm, we computed the fractional part of the determined positional coordinates as shown in Figs. S2a-c. Neither of the three coordinates shows a strong deviation from a flat distribution. We also computed the distributions of the absolute value of the three components of the orientation vector $\hat{\mathbf{u}}$, see Figs. S2d-f. The distributions are not completely flat, which is not surprising considering the limited number of pixels per particle and the effect of the (theoretically approximated) PSF. These deviations, however, did not hamper an accurate determination of the rotational motion of the particles. Fig. S2g
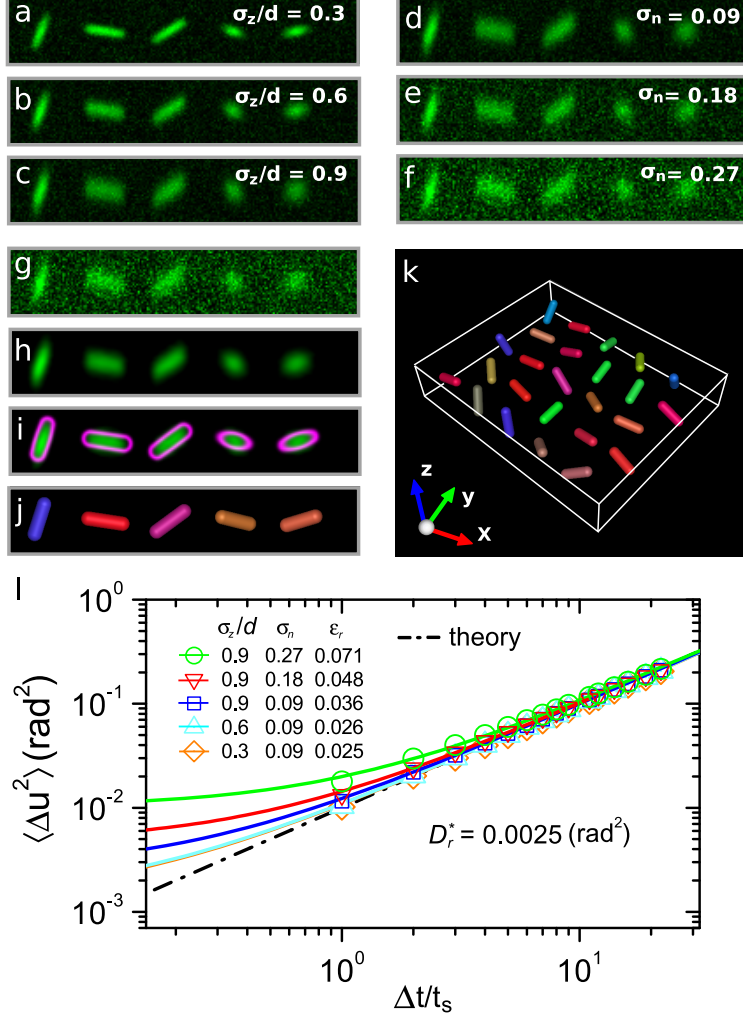
FIG. 1. The effect of z-resolution (σ_z) and noise (σ_n) on the measurement of rotational motion. To study this effect, test-images were generated with 25 randomly rotating particles fixed on a lattice. (a-c) The effect of a decrease in z-resolution (increase in σ_z). (d-f) Increase in noise level σ_n. (g) Original test-image with $\sigma_z/d = 0.9$ and $\sigma_n = 0.27$. (h) The image after filtering and (i) after particle fitting. (j,k) Computer rendered particles with color coding based on their orientation. (l) Mean squared angular displacement (MSAD) for decreasing σ_z/d and σ_n. The measurement error ϵ_r decreases for decreasing σ_z/d and σ_n.

shows the mean squared displacement (MSD) expected from theory and the corresponding result after particle tracking. The statistical errors for the individual measurement points are smaller than the symbol size. From the fit to equation (4) in the main paper, we obtain $D_t^* = (1.021 \pm 0.004) \times 10^{-2}$ and $\epsilon_t/d = (5.47 \pm 0.01) \times 10^{-2}$. In Fig. S2h, results are shown for the mean squared angular displacement (MSAD). Fitting to expression (5) in the main

4

paper results in $D_r^* = (5.06 \pm 0.06) \times 10^{-3}$ rad^2, which recovers the imposed theoretical value, and results in a small static orientation error of $\epsilon_r = (1.2 \pm 0.1) \times 10^{-2}$ rad.
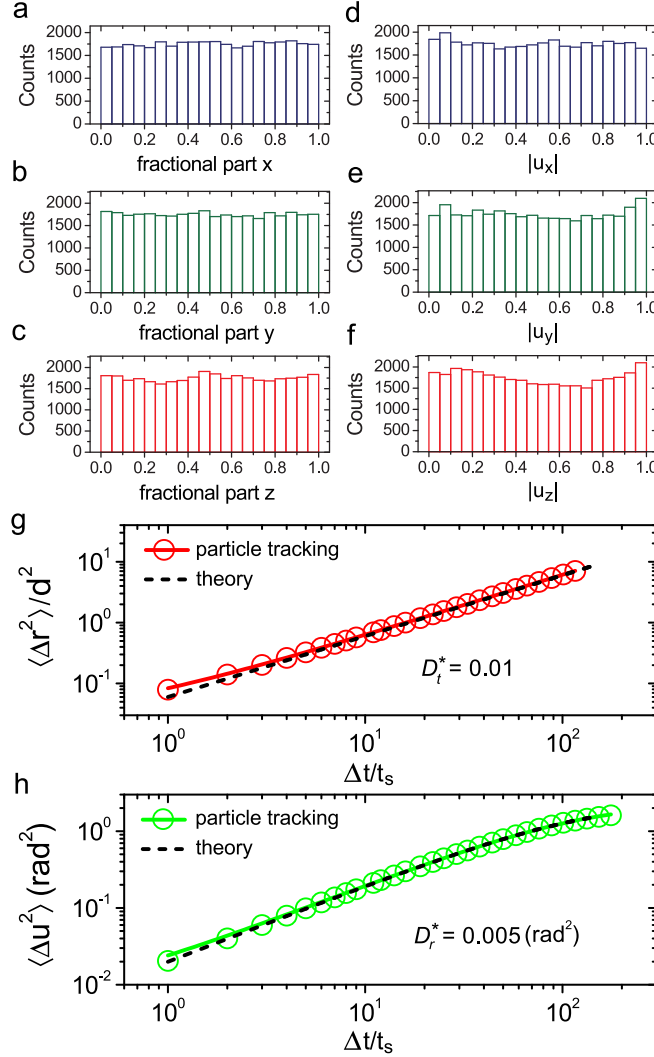
FIG. 2. Tracking results from computer generated 3D test-images of single, freely diffusing particles. (a-c) The fractional parts of the positional coordinates do not show signs of significant pixel-bias. (d-f) The absolute value of the components of the orientation vector also do not indicate any strong orientational bias. (g) Mean squared displacement (MSD) of the centre-of-mass of the particles. (h) Mean squared angular displacements (MSAD). We retrieved the correct translational and rotational diffusion coefficients with small static errors ϵ_t and ϵ_r respectively. The statistical errors for the individual measurement points are smaller than the symbol size and the black dashed lines are expected from theory.